CERN – European Organization for Nuclear Research

European Laboratory for Particle Physics

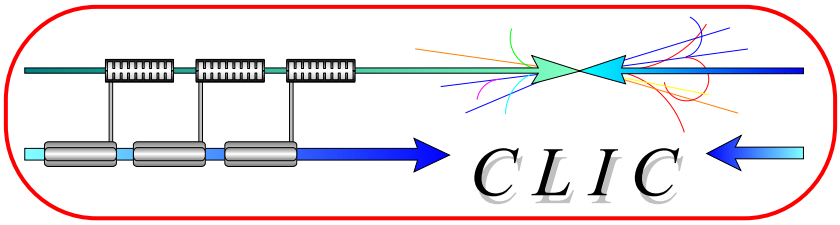

CLIC Note 460

USER GUIDE FOR WAKE

A.J. Riche

Abstract

WAKE is a code simulating multi-bunch, multi-particle beams in linac with wakefields having high group velocity. The group velocity complicates the calculation because of the constant relocation of the particles creating the field and because the path length of a particle within the field of a preceding particle is not the length of the RF structure, but depends on the distance between the particles. It is the potential, i.e. the product of the field and the path length which is considered, rather than the field itself. In order to account for the varying positions of the particles, the structure is divided into intervals at the end of which the potentials are calculated. To save time, summing the potentials is not repeated, but the vector sum is transformed by the difference in phase when a particle replaces the preceding one at the same section end. A complementary update is necessary because the transverse positions have changed. The equations of the dynamics are then applied. In addition to this specific treatment for the wakefields, more conventional operators for travelling wave acceleration and focusing are provided. The focusing forces may be automatically adjusted for a decelerator or given at each focusing element. The input list is simple and one can select output graphics representing the results of the longitudinal and the transverse motions for the whole beam train, or for groups of particles. The code, written in FORTRAN 77, is the result of years of studies of the CLIC decelerator and of the CTF accelerator and decelerator. It has been tested against experimental measurements in CTF. Examples are given for these machines.

Geneva, Switzerland
27 September 2000

USER GUIDE FOR WAKE

J.A. Riche
Cern, Geneve, Swizerland

WAKE is a code simulating multi-bunch, multi-particle beams in linac with wakefields having high group velocity. The group velocity complicates the calculation because of the constant relocation of the particles creating the field and because the path length of a particle within the field of a preceding particle is not the length of the RF structure, but depends on the distance between the particles. It is the potential, i.e. the product of the field and the path length which is considered, rather than the field itself. In order to account for the varying positions of the particles, the structure is divided into intervals at the end of which the potentials are calculated. To save time, summing the potentials is not repeated, but the vector sum is transformed by the difference in phase when a particle replaces the preceding one at the same section end. A complementary update is necessary because the transverse positions have changed. The equations of the dynamics are then applied. In addition to this specific treatment for the wakefields, more conventional operators for travelling wave acceleration and focusing are provided. The focusing forces may be automatically adjusted for a decelerator or given at each focusing element. The input list is simple and one can select output graphics representing the results of the longitudinal and the transverse motions for the whole beam train, or for groups of particles. The code, written in FORTRAN 77, is the result of years of studies of the CLIC decelerator and of the CTF accelerator and decelerator. It has been tested against experimental measurements in CTF. Examples are given for these machines.

I. INTRODUCTION

A particle with longitudinal speed c interacts with a structure when crossing it. The field of the interaction propagates behind the 'leading' particle L, with group velocity v_g from all the positions of its trajectory. We consider only structures with $v_g>0$. The 'test' particle T coming behind L at speed c overtakes the field L had generated when it was at the entrance of the structure, and then the fields L had generated further on. Therefore the length of the path along which the fields are applied to T is different from the length of the structure itself. Moreover, as the test particle progresses along the structure, the number of the leading particles varies. Each of them creates a different field on T, and the length of the path along which the field applies is also different. To simplify the calculations, the structure is divided into intervals. At the end of each interval, the leading particles are identified, and the field, the path length on T, and the potential for each leading particle are evaluated. Then the motion of T is calculated. Two consecutive 'test' particles, separated by Δt, arrive at the end of the same interval. A group of particles leads both T_2 and T_1, but with distances differing by $\Delta t/c$. The sum of the potentials on T_2 can be directly derived from the one on T_1, with a correction to take into account those leading particles which are not in common.

In WAKE, each bunch is longitudinally divided into slices with distributed charges, each slice into energy bins to simulate an initial incoherent energy distribution, each bin into 'macro-particles' to account for the emittance. The equation of the transverse motion x under the influence of resonant mode 1 wake field contains in its right hand side the sum of the forces of the leading particles. The charge-weighted addition of the equations for the particles T_i of the same energy bin in a slice gives the equation for the average $\langle x_i \rangle$. The difference of this equation with the one of x_i gives the equation for the betatron motion

around the trajectory obtained for the average. The envelope is therefore known[1]. For the other modes, the envelope is obtained by tracking many trajectories.

In chapter 2, the role of the group velocity is analyzed. The potentials are calculated and the equations for the particle dynamic are set for particles in structures with full rotational symmetry, or with rotational symmetry modulo $2\pi/m$ (CLIC drive beam). Then a solution is proposed for matching the focusing to the huge energy spread of the particles along a decelerator. Chapter 3 describes the input data setting. Some output graphs for the CLIC studies are shown in chapter 4. The field formulation for symmetrical structures is recalled in Appendix 1, for completion. Examples of input data for CTF and for the CLIC decelerator are given in Appendix 32 to 4.

II. DYNAMICS IN A STRUCTURE

II.1 ROLE OF GROUP VELOCITY

Test particle T crosses the structure at distance s behind leading particle L, at the same speed c. The distance to the entrance of the structure is represented versus time in Fig.1, in which c and group velocity $v_g>0$ are quoted instead of the tangents of the angles. The power of the interaction of L with the structure propagates towards the exit of the structure at speed v_g <c. Therefore the field at particle T from particle L is that emitted when L was at L'. At that time, T was at T'. The total path length of T in the field is needed for evaluating the potential. It is not the total length l_c of the structure, but $l = l_c – s\ v_g / (c- v_g)$, because T has to overtake the field of L.

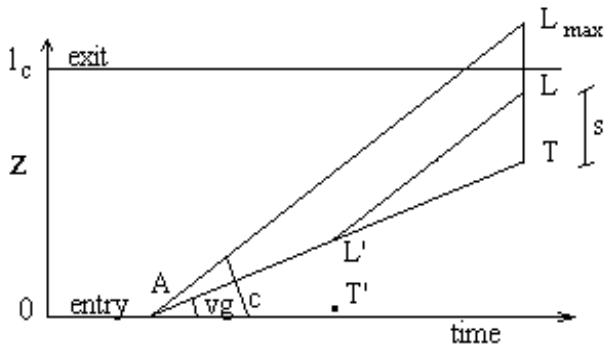

FIG. 1. Role of group velocity

Shifting back in z the triangle L' T L until L' is on the z=0 axis gives the first position of T in the field of L and then the path length l.

II.2 WAKE FIELDS AND POTENTIALS FOR CYLINDRICALLY SYMMETRIC STRUCTURES

The effect of the potential on the dynamics of particle T for an interval is evaluated by applying an impulse matrix on the (x, p_x) vector coordinates if the force varies in proportion with the position x. If this is not the case, the (x, p_x) vector is transformed by a kick on p_x. This kick may me applied at any end of the interval of shared between both ends.

II.2.1 Mode 0 wake field: longitudinal momentum change and radial effects

Using ω_0 and k_0 for the frequency and loss factor, q_i for the charge of the leading particle L_i, the longitudinal wake field at a test particle T behind L_i is[2]:

$$E_{z,i} = -2\, q_i\, k_0 \cos(\omega_0\, s_i / c) \qquad (2)$$

The potential change is evaluated each time T crosses an interval Δl of the structure, by the application of the wake field forces due to particles L_i along path length $\Delta z_i \leq \Delta l$ specific to each of them. The momentum change is:

$$\Delta (\beta\gamma)_z = (e / m_0 c^2)\, \Sigma_i\, \Delta z_i\, E_{zi} \qquad (3)$$

All these longitudinal fields also have a radial effect that can be accounted for as follows.

A travelling wave matrix M gives the transverse effect of the field averaged over Δl:

$$\begin{matrix} 1 & \mathrm{Ln}\,[1 + \Delta(\beta\gamma)_z / (\beta\gamma)_z]\;\; \Delta l\;\; (\beta\gamma)_z / \Delta (\beta\gamma)_z \\ 0 & (\beta\gamma)_z \;/\; [(\beta\gamma)_z + \Delta(\beta\gamma)_z] \end{matrix} \qquad (4)$$

An impulse matrix M_e gives the effects of the gradient of the field obtained with the difference $\Delta E_z = E_{zk} - E_{zk-1}$ of the longitudinal potentials between the limits of an interval k:

$$\begin{matrix} 1 & 0 \\ -\,[e/m_0 c^2]\, \Delta E_z / [2/(\beta\gamma)_z] & 1 \end{matrix} \qquad (5)$$

This is because, by the conservation of the magnetic flux, the radial potential associated with ΔE_z is:

$$\Delta z\, E_x \sim -\,(x / 2)\, \Delta E_z$$

and the radial momentum change is:

$$\Delta (\beta\gamma)_z = -\,[e/m_0 c^2]\, \Delta E_z\, x / [2/(\beta\gamma)_z]$$

The effect is applied at the entrance of the interval. For the first interval, $(E_z)_{i-1} = 0$. At the last interval, the field returns to zero, the matrix is multiplied by an impulse matrix, with E_z replacing $-\Delta E_z$.

II.2.2 Mode 1 radial wake field

The longitudinal field is neglected. The radial wake field due to particle L of charge q displaced by x_q from the axis is damped. For the propagation time between L' and T (Fig.1), the damping term d and the x projected field E_x are:

$$d = \exp\,[\, -\omega_1\, t / (2\, Q)] = \exp\,[\, -\omega_1\, s / (2\, Q\, (\, 1 / v_g - 1 / c\,)\,)\,]$$

$$E_x = 2\, q\, (x_q / a)\, [c / (\omega_1\, a)]\, k_1 \sin(\omega_1\, s / c) \exp\,[\, -\omega_1\, s / (2\, Q\, (\, 1 / v_g - 1 / c\,)\,)\,] \qquad (6)$$

The potential resulting from all L'_i is calculated with the corresponding field and path length. Then, it is distributed into two equal kicks at the ends of the interval.

.

II.3 RECURRENCE OF FIELDS AND POTENTIALS AT ENDS OF INTERVALS

The beam progresses by a fixed distance Δs between two consecutive test particles T_1 and T_2 as observed at the end of the interval n. T_1 and T_2 see the common wake field effect of particles that are in front of them. However the potential seen by T_2, is that seen by T_1 plus the modification due to the rotation $\omega \Delta s / c$ of the phase. It is also necessary to add the action of particle T_1, which is a new leading particle for T_2 and to remove that of the particles whose fields have left the interval.

II.3.1 Fields

Using the brief complex notation, the longitudinal field of the mode 0 is summed on p particles that are leading T_1:

$$E_{z'T1} = -2 k_0 \mathbf{P}\{\Sigma_{i=1,p} q_i \exp (\imath \omega_0 s_i / c)\} \quad (7)$$

Therefore, the field due to the same particles on T_2 is:

$$E_{z'T2} = \mathbf{P}\{ \exp \imath (\omega_0 \Delta s / c) \mathbf{E}_{z'T1}\} = \cos (\omega_0 \Delta s / c) \mathbf{P}\{\mathbf{E}_{z'T1}\} - \sin (\omega_1 \Delta s / c) \mathbf{I}\{\mathbf{E}_{z'T1}\} \quad (8)$$

By including the particle T_1 itself in the sum, T_1 is taken as a leading particle for T_2. The self-field, that is $- k_0 q_0$, should be removed from the sum for the calculation of the dynamics.

Similarly, for mode 1, the transverse wake field on T_2 is calculated from the field on T_1, with

$K_1 = k_1 c / (\omega_1 a^2)$,

$$E_{x'T1} = 2 K_1 \mathbf{I}\{\Sigma_{i=0,p} x_i q_i \exp (\imath \omega_1 s_i / c) \} \exp -[\omega_1 s_i / (2 Q (1/c-1/v_g))] \quad (9)$$

$$E_{x'T2} = \mathbf{I}\{ \exp \imath (\omega_1 \Delta s / c) \mathbf{E}_{x'T1} \} \exp -[\omega_1 \Delta s / (2 Q (1/c-1/v_g))] \quad (10)$$

II.3.2 Potentials:

Suppose first that the wake potential is only calculated when particle T_1 is at the end of the last interval, that is at $l_s = n \Delta l$. The path length for the field of L_i is: $n \Delta l - s_i v_g /(c - v_g)$. As we include the particle T_1 itself, the longitudinal potential P_z due to p leading particles is:

$$P_{z'T1} = -2 k_0 \Sigma_{i=0,p} \{q_i \cos (\omega_0 s_i / c) [n \Delta l - s_i v_g / (c - v_g)] \} \quad (11)$$

It is easy to show that the potential on T_2 is obtained from the potential on T_1 by:

$$P_{z'T2} = E_{z'T2} n\Delta l - \mathbf{P}\{\mathbf{AP}_{z'T2}\} v_g / (c - v_g) \quad (12)$$

where $\mathbf{AP}_z$ is some kind of 'auxiliary' potential defined with s_i :

$$\mathbf{AP}_{zT1} = -2\, k_0 \Sigma_{i=0,p}\ [\, q_i \exp(\imath\, \omega_0\, s_i / c)\, s_i\,] \qquad (13)$$

The iteration from T_1 to T_2 is simply achieved by transforming s_i to $s_i + \Delta s$:

$$\mathbf{AP}_{zT2} = \Delta s\, \mathbf{E}_{zT2} + \exp \imath\, (\omega_1\, \Delta s / c)\, \mathbf{AP}_{zT1} \qquad (14)$$

giving the longitudinal potential update (12). The radial potential P_x is:

$$P_{xT1} = 2\, K_1 \Sigma_{i=0,p}\, \{q_i\, x_i \sin(\omega_1 s_i / c)\, [n\, \Delta l - s_i\, v_g / (c - v_g)] \exp -[\omega_1\, s_i / (2Q(1/c - 1/v_g))]\ \} \qquad (15)$$

A similar iteration of an 'auxiliary' radial potential $\mathbf{AP}_x$ defined with s_i is used:

$$\mathbf{AP}_{xT1} = 2\, K_1\, \Sigma_{i=0,p}\, \{\, q_i\, x_i \exp(\imath\, \omega_1\, s_i / c)\, s_i \exp -[\omega_1\, s_i / (2Q(1/c - 1/v_g))]\ \} \qquad (16)$$

Its update differs from the one of $\mathbf{AP}_z$ because writing (15) instead of (11) involves a sine to cosine substitution and a multiplication by the damping term: $\exp -[\omega_1\, \Delta s / (2Q(1/c - 1/v_g))]$. The updated radial potential on particle T_2 is finally:

$$P_{xT2} = I\{\mathbf{E}_{xT2}\}\, n\, \Delta l \ - I\{\mathbf{AP}_{xT2}\}\, v_g / (c - v_g)]. \qquad (17)$$

II.3.3 Division of structure in n intervals

Consider particle T at the end of interval n. The potential gained by T in interval n depends on the fields due to leading particle L_i and on the common part l_{LTi} of the path length $n\Delta l - s_i v_g/(c - v_g)$, with an interval Δl. Fig.2 shows T at the end of interval 2, L at distance Δs in front of T, and L' in interval 2. In this case, the common part of the path length of T with interval 2 is the interval 2 itself. The leading particles are separated into 2 classes: 'A' if $l_{LTi} = \Delta l$, and 'B' if $l_{LTi} < \Delta l$. Accordingly, the sum of the fields on T are separated into 2 terms E_A and E_B, with the same expressions as in the preceding paragraph, but with indices $i \in A$ or $i \in B$ instead of i=0,p. The sum of the potentials are also separated into P_A and P_B. P_A is the product $\Delta l\, E_A$. The update of P_B is made according to the above equations.

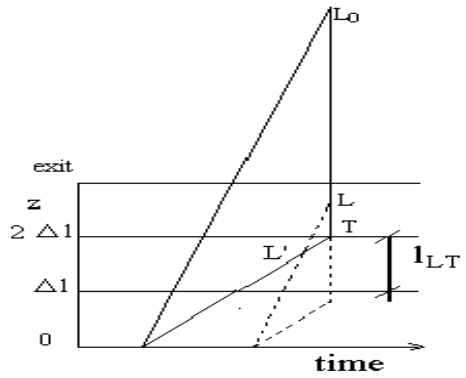

FIG.2. Path length l_{LT}. T is at end of interval 2. Point L' is not in interval 1 so $l_{LT} = \Delta l$ (class A)

When T2 replaces T1 at the end of interval 2 (Fig.2), leading particle L progresses also by Δs. Therefore, some of the leading particles of class B for T_1 are in class A for T_2. Their individual field and potential contribution for T_1 should be recalculated, removed from stacks B, calculated for the new path length for T_2, and added to stacks A. In addition, some particles are only removed, because their fields have left the structure.

Transverse co-ordinates are recorded at the limits of the intervals. Transverse mode 1 fields and potentials depend on the co-ordinates x_i of the leading particles L_i. The sums in stacks A and B are updated by substitution of fields and potentials due to L_i with the new values of x_i each time the corresponding point L'_i crosses a limit of an interval.

These substitutions and removals can be resumed as follows:

When considering T_2 after T_1, both types of stacks are updated. In addition, L' may cross the limit of an interval. These limits may be:

- 1. the upper limit, but not of the first interval. Substitution in stacks B is made for the radial fields and potentials recalculated with previous and the x transverse positions.

- 2. the upper limit of the first interval. The field and the potential are recalculated with path length Δl, removed from B stacks, calculated again with the path length l_{LT} and added in A stacks. For the dipole mode, the calculations are made with proper x positions.

- 3. the entrance of the structure: the field and potential due to L' are recalculated with path length l_{LT} with transverse position at interval 1, and removed from A stacks.

II.4 WAKE FIELDS FOR STRUCTURES WITH CYLINDRICALLY SYMMETRY MODULO 2 PI / M

For collecting the 30 GHz power, the decelerating structures have m longitudinal slits along their core, generating a modulo $2\pi/m$ symmetry[3]. Calculations with MAFIA and measurements[4] show that mode 0 and mode 1 wake fields are combined with multiple mode fields depending on the (r, ϕ) co-ordinates of T in the symmetry axis:

$$E_z = 2\, q_i \cos(\omega_0 s_i / c) \sum_j k_j (r/a)^{m\,j} \cos(m\, j\, \phi) \qquad (18)$$

The Panofsky and Wentzel theorem[5] gives the mode m transverse field behind L_i as:

$$\mathbf{E_t} = E_r + \imath\, E_\phi = -2\, q_i \sin(\omega_0 s_i/c) \sum_j k_j (r/a)^{m\,j-1} (m\, j/a)\, (c/\omega_0)\, [\mathbf{r} \cos(m\, j\, \phi) - \phi \sin(m\, j\, \phi)] \qquad (19)$$

The unit vectors for the test particle are $\mathbf{r}$ and ϕ. If x and y are the co-ordinates of T:

$$E_x = 2\, q_i \sin(\omega_0 s_i/c) \sum_j k_j (x/a)^{m\,j-1} (m\, j/a)\, (c/\omega_0) \cos[(m\, j-1)\, \phi] \qquad (20)$$

$$E_y = -2\, q_i \sin(\omega_0 s_i/c) \sum_j k_j (y/a)^{m\,j-1} (m\, j/a)\, (c/\omega_0) \sin[(m\, j-1)\, \phi] \qquad (21)$$

The recurrence on the potentials is similar to the recurrence shown for resonant modes 0 and 1.

II.5 FIELDS FROM EXTERNAL SOURCES

This field is described in the data for a particle on the crest of the voltage, and approximated linearly by a succession of segments. A description with 2 segments for each cell seems convenient. Phases for the successive bunch heads are given. As particle's speed is c, the phases for all particles are known. On Fig.3 are represented the field E_z, with an arbitrary scale (plain line) in 16 cells of a structure, $\beta\gamma$ and the x trajectory for a particle entering aside the structure axis, with 0 slope in the plane containing the initial momentum and the axis.

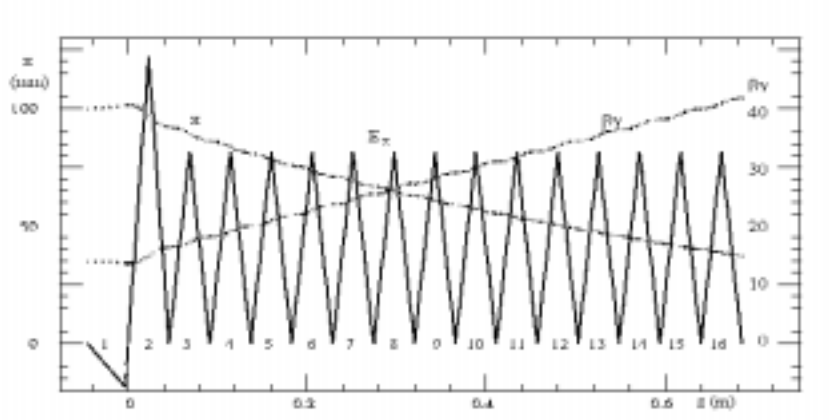

FIG.3 External source field in 16 cells of a TW structure (plain, arbitrary scale), momentum and off-axis trajectory (dotted)

II.6 IMPLICIT VARIATION OF THE FOCUSING

If the initial energy spread in the beam is small, the best focusing is found by choosing the focusing forces at each quadrupole for the particle with the smallest energy[6]. The trajectory of a particle of momentum p in a linac with FODO focusing of mesh length L is represented in a diagram (Fig.4), which co-ordinates are the focal length F = p/(q Gl) of the focusing quadrupole with integrated force Gl and the TWISS function β_F (F,L). One has to choose the details of the lattice. Keeping equal phase advance per mesh, the trajectory is a straight line in the diagram (Fig.4):

$$\beta_F (F, L) = 2 F [1+\sin (\mu/2)]^{1/2} / [1-\sin (\mu/2)]^{1/2} \qquad (22)$$

Keeping constant the distance L between the quadrupoles, it is a curve on the same figure.

$$\beta_F (F, L) = 2 F (F+L/2))^{1/2} / (F-L/2))^{1/2} \qquad (23)$$

Only slow variation of parameters along the linac is allowed. For any choice, at a given point in the linac, L and Gl are fixed. The particles with different momenta at that point are represented by a segment of a line with constant L. The normalized emittance ε is constant, the transverse position of the particle is:

$$x = \beta_F \varepsilon / p \qquad (24)$$

According to the previous expression, for L and Gl given, β_F /p is a decreasing function of p:

$$\beta_F /[p/q\ Gl] = 2\,[p/q\ Gl + L/2]^{1/2} / [p/q\ Gl - L/2]^{1/2} \qquad (25)$$

In other words, the maximum envelope x is obtained for p minimum (point M on Fig.4). All the other particles at the same location in the linac, have smaller transverse positions, even if their β_F values are higher (as it may happen on the right of point M, in Fig.4). As the particle with the minimum energy has the maximum transverse position, it is enough to choose the line representing the trajectory of the particle with the lower energy such that it stays away from the instability occurring at F=L/2, for μ=180. One choice could be to keep the same value of L all along the linac.

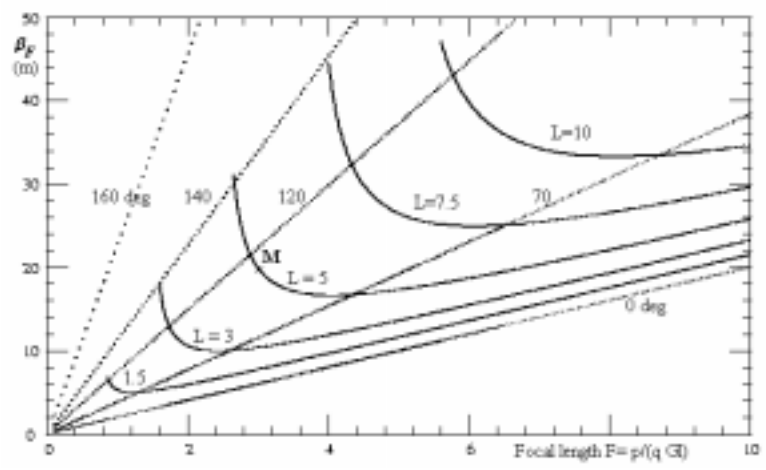

FIG.4 TWISS β_F parameter and phase advance μ at a QF quadrupole as a function of focus length F

For a more rigorous proof, consider the coefficients "a" of a transport matrix built for conjugate variables (x, q $=p_x$ dx/ds), for a periodic system like a FODO mesh. From one reference plane to the following one (quadrupoles with identical position in successive meshes), the quadratic form:

$$-a_{21}\,x^2 + (a_{11}-a_{22})\,x\,p_x + a_{12}\,p_x^2 = U \qquad (26)$$

is invariant. The coefficients are changing with the energy parameter. If the variation with the energy is slow, the ellipse area is conserved. The area is invariant for all z (i.e. all

reference planes along the linac), for a particle with a given rank in the train. It is also invariant for a particle with a different rank, with another energy variation along the linac. But all these particles had the same momentum value p_0 at origin (see Fig.5) and the same initial emittance: the invariant concerns all particles at all places in the beam. With these conditions, the maximum envelope is found for the particles with minimum momentum p. Then, if the focusing is organized for the minimum p at all the quadrupole settings, all particles will be contained in the envelopes found for p_{min}[7].

If p_{min} (0) and Gl (0) are respectively the values found for the minimum momentum and the integrated gradient in a focusing quadrupole in the first mesh of the lattice, the integrated gradient in a corresponding quadrupole of a further mesh is:

$$Gl\ (z) = Gl\ (0)\quad [p_{min}\ (z)\ /\ (p_{min}\ (0)] \tag{27}$$

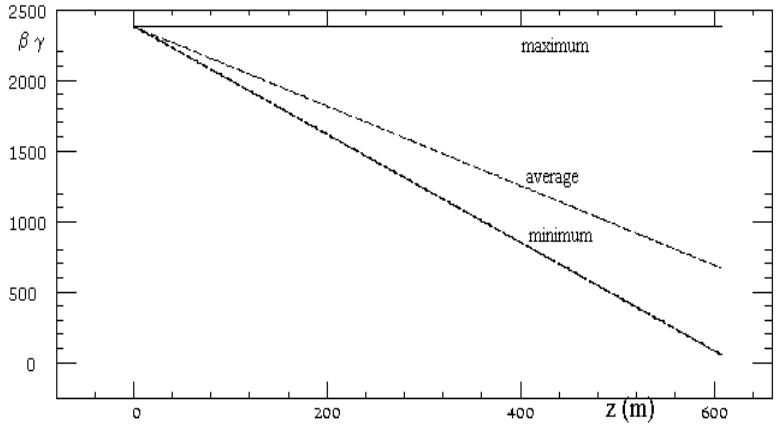

FIG.5. Momenta along a decelerator

III. INPUT DATA

The input data set is self explanatory, because a comment card precedes each card holding parameters. Input data are divided into 4 chapters:

III.1 BEAM PARAMETERS

At start, all bunches have the same normalized transverse emittance and Twiss parameters. The charge per bunch and their energy may be different between bunches or groups of bunches. The distribution within bunches is gaussian. The number of sub-slices helps to follow 5 bins of energy from an initial intra-slice energy distribution.

There is the possibility to specify the parameters for each bunch on an auxiliary file else than the data file. This option is chosen by setting a flag to 1 in the data file, as shown by the example, and by providing in the auxiliary file as many double cards as there are bunches, with:

bunch index, $\beta\gamma$, σ_x, $\langle x\, x' \rangle$, $\sigma_{x'}$,

bunch index, $\beta\gamma$, σ_y, $\langle y\, y' \rangle$, $\sigma_{y'}$, where x' is for dx/ds.

III.2 STRUCTURES

Different type of structures may be specified. A line of comments precedes each line, which lists parameters. A structure with $v_g \sim 0$ may be divided into smaller structures. This is not possible if v_g differs from 0, because of the physical reasons mentioned above. The number of intervals for a division internal to the process should be indicated. One always gives modes 0 and 1 frequencies and amplitudes. For structures with modulo $2\pi/m$ symmetry, one gives first the number of multiples specified, and, if this number is not 0, as many values for jm and amplitudes as required.

If the field in the structure depends on an external source, this field must be specified at the limits of each step and at the end of the last one, for the particle which sees the maximum field. The phase, relative to this field, of the first slice of bunch 1, and the phase shift per bunch should be given for the exact calculations of all slices of all bunches.

III.3 ERRORS

Only errors in relation with a systematic transverse displacement of the structures are implemented in present version.

III.4 INSTRUCTIONS FOR PLOTTED OUTPUTS

There are 2 sorts of plots:

- Plots at a given z position along the beam line (local plot).

These positions are indicated in the description of the lattice by code '51.0'. One may plot:

$\beta\gamma$, x, y, as a function of the slice numbers for one or several bunch chosen a priori

$\beta\gamma$ function of the bunch number, dx/ds versus x, dy/ds versus y, for slices of selected bunches, but given the step for the series of slices.

- Plots along the beam line. One may plot:

$\beta\gamma$, x or y (mean, maximum and minimum values), or, with specification of the bunch step, the first bunch, the last bunch, the step for the slices:

x or y envelopes or dx/ds or dy/ds averaged for the slice. This may be required with all bunches trajectories superposed or with one bunch per page.

III.5 LATTICE AND COMMANDS

There is a line for each of the elements of the lattice, unless repetition of a list of element is required between specified beginning and end of a loop. The first parameter of an element is the type code, second and third parameters are the length and the field parameter. The forth parameter gives the index of the group the element belongs to. A line may also contain a command as shown below.

Lattice

Code	Parameter 1	Parameter 2	Parameter 3	Comment
3.	Length (m)	dummy	Dummy	Drift
5.	Length (m)	Integrated gradient (T)	Quadrupole index	Quadrupole
11.	dummy	dummy	Dummy	Structure
20.	Angle (deg)	"	"	Rotation
9.	Nb. of iterations	"	"	Begin iterat. Loop
9.	0.	"	"	End iterat. Loop
50.	dummy	"	"	Save for plot
51.	"	"	"	Local plot
60.	"	"	"	Plot along b. line
70.	Bunch 1	Bunch 2	"	Printed statistics
0.	0	0	0	End of lattice

IV. RESULTS

In the CLIC 2 beams accelerator principle[8], the 30 GHz power is extracted from the structures loaded by the bunches of the decelerator beam and guided to the accelerating structures of the main beam which is installed parallel with the decelerator. Some results obtained for the dynamics in both CTF and CLIC decelerator are presented below.

Fig.6 shows the 2 σ envelopes along the CLIC Test Facility beam line for all the particles of a train with 48 bunches, when a systematic 0.5-mm transverse displacement of the structures is simulated. Irises limiting the aperture are indicated. The 8 nC charge per bunch is transmitted for all bunches, while the 13.5 nC charge is stopped on the iris of structures 3 and 4 [9].

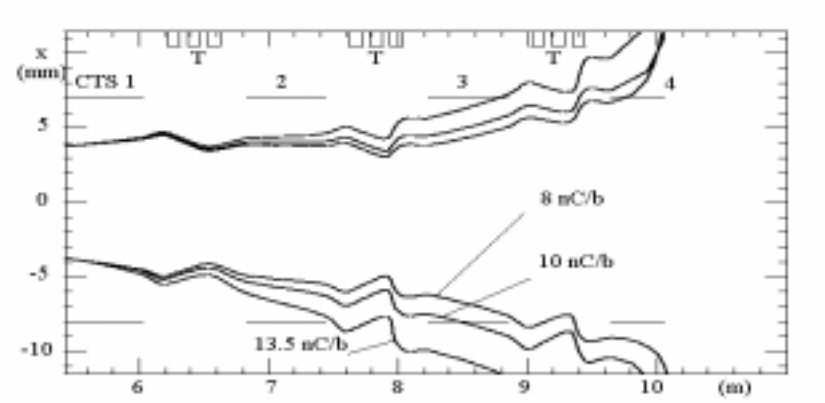

FIG.6 X-projection envelope for all bunches in CTF decelerator, for 8 to 13.5 nC/ bunch

Envelopes for each of the energy bins of each slice of a bunch may be plotted as in Fig.7. Envelopes for 2 σ of the 5 energy bins of the first slice are intercepted by the iris of decelerating structures ' CTS 3' and 'CTS 4'. The rest of the beam is distorted, but reaches the end line charge monitor.

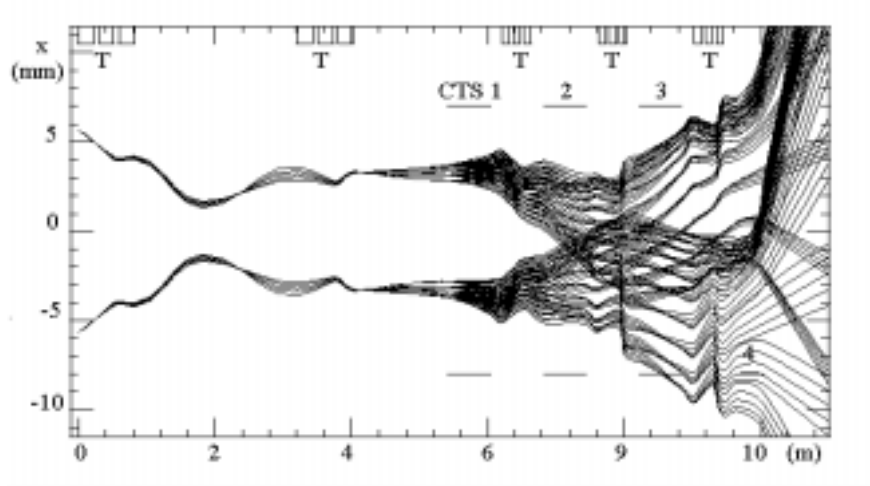

FIG.7 Bunch transverse envelope in CTF (10 nC/b). The envelopes are shown for each of the 5 energy bins of each slice

The momentum decrease along the CLIC drive beam is shown in Fig.5. Group velocity, bunch distance and structure active length determine the number of bunches (about 50) involved in building the wake. With focusing adapted to the minimum energy at each quadrupole, and if the effect of the transverse wake field is low, the transverse beam size stays small until the kinetic energy of some particles approaches 0. Momentum and momentum spread at that point are shown Fig.8.

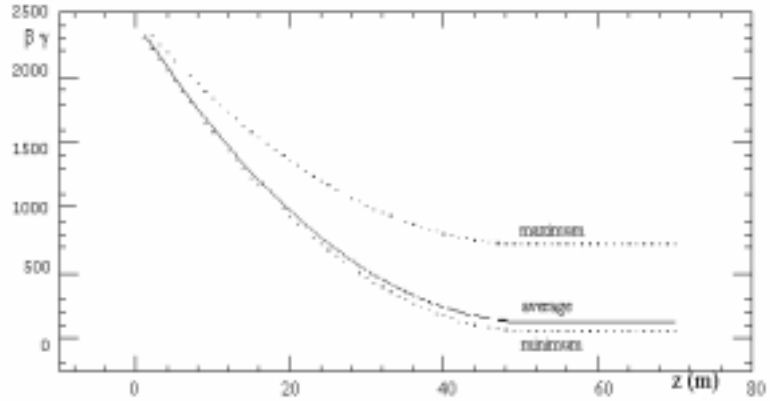

FIG.8 Extremum and average momentum at CLIC decelerator end

The 2 σ envelope recorded at the quadrupoles is shown in Fig.9 for the beam train. A beam transverse offset of 0.1 mm at the entrance of the CLIC decelerator line is the source of the transverse field. The decelerator contains 530 structures.

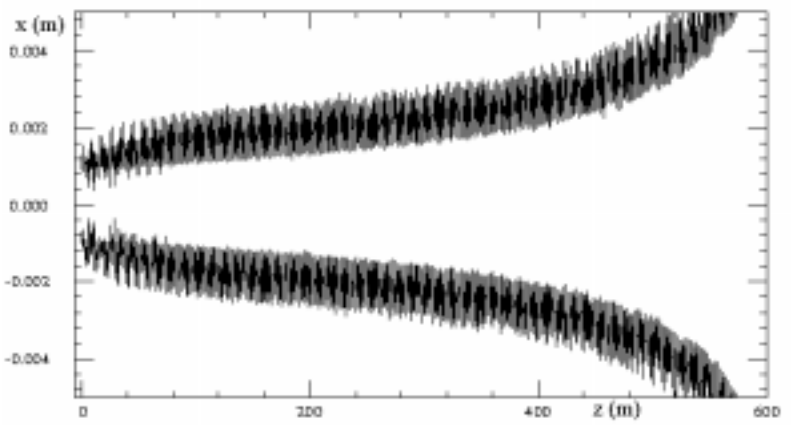

FIG.9 All beam X projected envelope along CLIC decelerator

IV. CONCLUSION

Group velocity gives some complication in the calculations because of the need for computation time economy. Precision requires dividing structures into intervals. Calculating the potentials with the more exact path length allows using a few intervals. An automatic matching of the quadrupole forces for the particles with the lowest energy gives the best focusing for decelerators like the CLIC 'drive beam'.

[1] S. Fartoukh in *Particle Accelerator Conference,* 1997, edited by IEEE, Piscataway, NJ, 1007.

[2] T. Weiland, R. Wanzenberg in *Joint US-CERN Accelerator School,* 1990, edited by M. Dienes, M. Month, S. Turner, (Springer Verlag, 1992).

[3] A. Millich, A. Riche, D, Schulte in *Particle Accelerator Conference*, 1999, *and* CERN/PS 99-028 (PP).

[4] G. Carron, A. Millich, L. Thorndahl in *International Computational Accelerator Physics Conference, Monterey,* 1998.

[5] W.H.K. Panofsky and W.A. Wenzel, Review Scientific Instruments **27**, p. 967 (1956).

[6] J.A.Riche, CERN, CLIC Note 334 (1997).

[7] The CLIC RF Power Source, CERN 99-06 (1999).

[8] J. P. Delahaye and al in *Particle Accelerator Conference,* 1999, edited by IEEE Accelerator conference, p. 250.

[9] R. Bossart, H.H. Braun, M. Chanudet-Cayla, G. Guignard, A. Riche, M.Valenti in *7th European Particle Accelerator Conference ,* 2000, *and* CERN/PS 2000-042 (PP)

APPENDIX I

A I. Fields for structures with cylindrical symmetry

The longitudinal wake field at a test particle distant by s from the leading point like charge q is the summation on the azimuthal mode of index m of the series:

$$E_z = -2\, q\, \Sigma_m \, (r_q / a)^m \, (r / a)^m \cos(m\,\phi) \, \Sigma_n \, k_{m\,n} \cos(\omega_{m\,n}\, s / c) \qquad \text{(AI.1)}$$

Index n is the resonant mode index and $\omega_{m\,n}$, $k_{m\,n}$, are the frequency and the loss parameters corresponding to the mode n and to index m.

a is the iris radius, r and r_q are respectively the test particle and the leading particles radii. The angle between the leading and the test particle is ϕ. The transverse wake is derived according to the theorem of Panofsky and Wentzel:

$$[\text{grad}\,(E_z)]_t + \partial\, E_t / \partial\, s = 0 \qquad \text{(AI.2)}$$

From which:

$$E_r = 2\ q \Sigma_m (r_q / a)^m (r / a)^{m-1} \cos(m \phi) \Sigma_n (m/a)(c/(\omega_{m,n}) k_{m,n} \sin(\omega_{m,n} s / c) \quad \text{(AI.3)}$$

$$E_\phi = 2\ q \Sigma_m (r_q / a)^m (r / a)^{m-1} \sin(m \phi) \Sigma_n (m/a)(c/(\omega_{m,n}) k_{m,n} \sin(\omega_{m,n} s / c) \quad \text{(AI.4)}$$

If $\mathbf{r}$ and ϕ are the orthogonal unit vectors in the x-y plane, with $\mathbf{r}$ pointing to test particle,

$$E_t = E_r + E_\phi = 2\ q \Sigma_m (r_q / a)^m (r / a)^{m-1} \Sigma_n (m/a) (c/(\omega_{n,m}) k_{n,m}$$
$$[\mathbf{r} \cos(m \phi) - \phi \sin(m \phi)] \sin(\omega_{n,m} s / c) \quad \text{(AI.5)}$$

As,

$$\mathbf{r} = e^{j\phi} \mathbf{r_q} \quad \text{(AI.6)}$$

$$\phi = j\ \mathbf{r} = j\ e^{j\phi} \mathbf{r_q} \quad \text{(AI.7)}$$

then:

$$\mathbf{r} \cos(m \phi) - \phi \sin(m \phi) = e^{j\phi} \mathbf{r_q}\ e^{-jm\phi} = e^{j(1-m)\phi} \mathbf{r_q} \quad \text{(AI.8)}$$

From these notations, let us recall the expressions for the azimuthal modes 0 and 1 :

- m=0:

$$E_z = -2\ q \Sigma_n k_{0,n} \cos(\omega_{n,0} s / c) \quad \text{(AI.9)}$$

According to the fundamental theorem of the beam loading, the 'self field' is:

$$E_z \text{ (self)} = -\ q \Sigma_n k_{0,n} \quad \text{(AI.10)}$$

There is no transverse wake.

- m=1:

$$\mathbf{E_z} = -2\ q\ (r_q / a) (r / a) \cos(\phi) \Sigma_n k_{1,n} \cos(\omega_{1,n} s / c) \quad \text{(AI 11)}$$

The longitudinal field exists only if leading and test particles are both off axis. This field is generally neglected, because it is small compared with longitudinal field for mode 0. From above relation, for m=1,

$$\mathbf{r} \cos(m \phi) - \phi \sin(m \phi) = \mathbf{r_q} \quad \text{(AI.12)}$$

$$\mathbf{E}_t = 2\ q\ (r_q / a)\ (c / (\omega_{1,n}\ a))\ \Sigma_n\ k_{1,n} \sin(\omega_{1,n}\ s / c)\ \mathbf{r}_q \qquad \text{(AI.13)}$$

The transverse field at the test particle is proportional with the shift of the leading particle from the structure axis

AII.CTF Input Data (decelerator part).

The input data list of cards contains groups made of a comment card and a card with parameters. For the cards describing the lattice there are no comments. There are also two titles which are followed by a comment cart: the general title, in format (3A8), and the titles 'Beam parameters', 'Structures', 'Plot Outputs', 'Lattice', which are in free format. In this way, the input set is self-explanatory. In the following are added the card number at beginning of the line.

(1) CTF 48 b., 13.5 nC/b, displ.++0.5mm, Trsv.Wake.On

(2) **********Beam Parameters

(3) Cinet.(eV) rms_x_norm_E(m r) β_x(m) α_x(m) rms_y_norm_E(m.r) β_y(m) α_y(m)

(4) 45.e+6 68.e-06 2.25 3.0 68.e-06 2.25 3.

(5) Envelope at N sigma, N=

(6) 2

(7) rms_bunch_l (m) rms_dE/E NSig_Cent_to_Edge NSig_Cent_to_dE/E_edge

(8) 0.65e-03 2.e-02 3 2

(9) Charge/bunch(C) Nbunc. Dist_b(cm) Nb_Slices Nb_Sub_Slices Nb_part/Sli.

(10) 13.5e-9 48 0.1 10 5 1

(11) Nb_bunches_per_group NG_groups

(12) 1 48

(13) Relative Charge in NG successive groups (up to 10 data per card)

(14) 1.0000 1.0000 1.0000 1.0000 1.0000 1.0000 1.0000 1.0000 1.0000 1.0000

(15) 1.0000 1.0000 1.0000 1.0000 1.0000 1.0000 1.0000 1.0000 1.0000 1.0000

(16) 1.0000 1.0000 1.0000 1.0000 1.0000 1.0000 1.0000 1.0000 1.0000 1.0000

(17) 1.0000 1.0000 1.0000 1.0000 1.0000 1.0000 1.0000 1.0000 1.0000 1.0000

(18) 1.0000 1.0000 1.0000 1.0000 1.0000 1.0000 1.0000 1.0000

(19) Relative Energy in NG successive groups (up to 10 data per card)

(20) 1.0000 0.9975 0.9950 0.9925 0.9900 0.9875 0.9850 0.9825 0.9800 09775

(21) 0.9750 0.9725 0.9700 0.9675 0.9650 0.9625 0.9600 0.9575 0.9550 0.9525

(22) 0.9500 0.9465 0.9450 0.9425 0.9400 0.9375 0.9350 0.9325 0.9300 0.9275

(23) 0.9250 0.9225 0.9200 0.9175 0.9150 0.9125 0.9100 0.9075 0.9050 0.9025

(24) 0.9000 0.8975 0.8950 0.8925 0.8900 0.8875 0.8850 0.8825

(25) If <> 0, Read on xxx.auxil on 2 lines (x then y): Index_Bunch , $\beta\gamma$, σ_x, <x x'>, $\sigma_{x'}$

(26) 1

(27) *********Structures

(28) Number of types of structures

(29) 2

(30) Structure_length (m) Structure iris radius (m) ********{Struct. Type 1}

(31) 0.6 0.0075

(32) Mode 0 Frequency

(33) 2.9979246e+10

(34) For Mode 0, write C if data=R'/Q circuitΩ/m, L if linac, V if loss factor(V/C/m)

(35) C

(36) Corresponding value (set it with – sign for load)

(38) -546

(39) Number of multipoles for 2 π/N fold symmetric structures (0 if symmetric)

(40) 0

(41) Mode 1 Frequency

(41) 2.997924e+10

(43) For Mode 1, write C if data=R'/Q circuitΩ/m, L if linac, V if loss factor(V/C)

(44) V

(45) Corresponding value

(46) 353.0e+12

(47) Group_velocity/c Q (attenuation)

(48) 0.53 100.

(49) Number of steps in structure

(50) 5

(51) External source field at beginning of each step + end of last step

(52) 0. 0. 0. 0. 0. 0.

(53) Phase shift bunch 1 (deg)

(54) 0.0

(55) d (Phase) per bunch

(56) 0.0

(57) Structure_length (m) Structure iris radius (m) ********{Struct. Type 2}

(58) 0.4 0.0075

(59) Mode 0 Frequency

(60) 2.9979246e+10

(61) For Mode 0, write C if data=R'/Q circuitΩ/m, L if linac, V if loss factor(V/C/m)

(62) C

(63) Corresponding value (set it with – sign for load)

(64) -546

(65) Number of multipoles for 2 π/N fold symmetric structures (0 if symmetric)

(66) 0

(67) Mode 1 Frequency

(67) 2.997924e+10

(68) For Mode 1, write C if data=R'/Q circuitΩ/m, L if linac, V if loss factor(V/C)

(69) V

(70) Corresponding value

(71) 353.0e+12

(72) Group_velocity/c Q (attenuation)

(73) 0.53 100.

(74) Number of steps in structure

(75) 5

(76) External source field at beginning of each step + end of last step

(77) 0. 0. 0. 0. 0. 0.

(78) Phase shift bunch 1

(79) 0.0

(80) d (Phase) per bunch

(81) 0.0

(82) Phase shift bunch 1

(83) 0.0

(84) Misalignments (m) rms and systematics

(85) Beam Offset xrms yrms x systematic y-systematics

(86) 0. 0. 0. 0.

(87) Quadrupoles 0 0 0 0

(88) Structures 0 0 0.5e-3 0.5e-3

(89) BPM 0 0 0 0

(90) Plots outputs **********

(91) Number of bunchs represented for plotting parameters at an element

(92) 3

(93) Identity of bunches represented for plotting parameters at an element

(94) 1 24 48

(95) At Elem. indicated by 50., for all Slices, βγ (slice) for selected b. =1:yes, =0: no

(96) 0

(97) At Elem. indicated by 50., for all Slices, x (slice) for selected b. =1:yes, =0: no

(98) 0

(99) At Elem. indicated by 50., for all Slices, y (slice) for selected b. =1:yes, =0: no

(11) 0

(101) At Elem. indicated by 50., for all Slices, βγ (bunch) for selected b. =1:yes, =0: no

(102) 0

(103) At Elem. indicated by 50., for all Slices, dx/ds versus x, for selected b. =1:yes, =0: no

(104) 0

(105) At Elem. indicated by 50., for all Slices, dy/ds versus y, for selected b. =1:yes, =0: no

(106) 0

(107) Along beam line :βγ, x y (max, min, average) set =1(yes) or =0 (no)

(108) 1 0 0

(109) Along beam line x envelope :Bunch step First bunch Last bunch Slice step

(110) 0 1 48 1

(111) Along beam line y envelope :Bunch step First bunch Last bunch Slice step

(112) 1 24 24 1

(113) Along beam line (1b./page) y envel. :Bunch step First bunch Last bunch Slice step

(114) 0 1 48 1

(115) Along beam line (1b./page) y envel. :Bunch step First bunch Last bunch Slice step

(116) 0 1 4 1

(117) Along beam line all traj slice x center :Bunch step First bunch Last b. Slice step

(118) 0 1 48 2

(119) Along beam line (1b/page) x cent per sl :Bunch step First bunch Last b. Sli. step

(120) 0 1 4 1

(121) Along beam line all traj slice y center :Bunch step First bunch Last b. Slice step

(122) 0 1 48 2

(123) Along beam line (1b/page) y cent per sl :Bunch step First bunch Last b. Sli. step

(124) 0 1 4 1

(125) Along beam, all <dx/ds> . slice traj. :Bunch step First bunch Last b. Slice step

(126) 0 1 48 1

(127) Along beam, (1b/page) <dx/ds> . sl. traj. :Bunch step First bunch Last b. Slice step

(124) 0 1 2 1

(125) Along beam, all <dy/ds> . slice traj. :Bunch step First bunch Last b. Slice step

(126) 0 1 48 1

(127) Along beam, (1b/page) <dy/ds> sl. traj. :Bunch step First bunch Last b. Slice step

(128) 0 1 2 1

(129)LATTICE **********

(130) 50.0 0. 0. 1.

(131) 51.0 1. 1. 1.

(132) 5.0 0.22 0.16104 1. !triplet after bunch compressor

(133)	50.	0.	0.	1.		
(134)	3.0	0.078	1.	1.		
(135)	5.0	0.22	-0.27445		2.	
(136)	50.0	0.	0.	1.		
(137)	3.0	0.078	1.	1.		
(138)	5.0	0.22	0.16852		1.	
(139)	50.0	0.	0.	1.		
(140)	3.0	1.0	1.0	1.		
(141)	50.0	0.0	0.0	1.		
(142)	3.0	1.399	1.	1		
(143)	50.0	0.	0.	1.		
(144)	5.0	0.22	0.30173		3.	!triplet in front of CTS1
(145)	50.0	0.	0.	1.		
(146)	3.0	0.078	1.	1.		
(147)	5.0	0.22	-0.38900		4.	
(148)	50.	0.	0.	1.		
(149)	3.0	0.078	1.	1.		
(149)	5.0	0.22	0.16049		5.	
(150)	50.0	0.	0.	1.		
(151)	3.0	0.869	1.	1.		
(152)	50.0	0.	0.	1.		
(153)	3.0	0.524	1.	1.		
(154)	50.	0.	0.	1.		
(153)11.		0.6	1.0	1.	!structure CTS1	

```
(154)  50.0   0.       0.              1.
(155)  51.    1.       1.              1.
(156)  3.0    0.1925   1.              1.
(157)  50.0   0.       0.              1.
(158)  5.0    0.095    0.31958                 6.      !triplet for CTS2
(159)  50.0   0.       0.              1.
(160)  3.             0.0615  1.      1.
(161)  5.0    0.095    -0.63578                7.
(162)  50.0   0.       0.              1.
(163)  3.             0.0615  1.      1.
(164)  5.0    0.095    0.31958                 8.
(165)  3.0    0.2095   1.0             1.0
(166)  50.0   0.       0.              1.
(167)  11.    0.6      1.0             1.      !structure CTS2
(168)  50.0   0.       0.              1.
(169)  51.    1.       1.              1.
(171)  3.             0.1925  1.      1.
(172)  50.0   0.       0.              1.
(173)  5.0    0.095    0.31958                 6.      !triplet for CTS3
(174)  50.0   0.       0.              1.
(175)  3.             0.0615  1.      1.
(176)  5.0    0.095    -0.63578                7.
(177)  50.0   0.       0.              1.
(178)  3.             0.0615  1.      1.
```

(179)	5.0	0.095	0.31958		8.
(180)	3.0	0.2095	1.01	0.	
(181)	50.0	0.	0.	1.	
(182)	11.0	0.6	1.0	1.	!structure CTS3
(182)	50.0	0.	0.	1.	
(183)	51.	1.	1.	1.	
(184)	3.0	0.1925	1.	1.	
(185)	50.0	0.	0.	1.	
(186)	5.0	0.095	0.31958		6.
(187)	50.0	0.	0.	1.	
(188)	3.	0.0615	1.	1.	
(189)	5.0	0.095	-0.63578		7.
(190)	50.0	0.	0.	1.	
(191)	3.0	0.0615	1.	1.	
(192)	5.0	0.095	0.31958		8.
(193)	50.0	0.	0.	1.	
(194)	3.0	0.2095	1.	1.	
(195)	50.0	0.	0.	1.	
(196)	11.	0.400	1.0	1.	!structure CTS4
(197)	50.0	0.	0.	1.	
(198)	51.0	1.	1.	1.	
(199)	3.	1.	1.	1.	
(200)	50.0	0.	0.	1.	
(201)	51.0	1.	1.	1.	

(202) 60. 0. 0. 1.

(203) 70. 1. 1. 1.

(204) 70. 21. 21. 1.

(205) 70. 48. 48. 1.

(206) 70. 1. 48. 1.

(207) 0.0 0. 0. 0.

AIII.CTF Input Data (CTF accelerator part, structure HCS).

The example is given to show a case with an external field source. As v_g ~0 in the structure, it can be segmented in several parts. In this case, the number of cells being only 13, there are as many parts as cells. Part1 describes the cell of HCS1, part2, the input coupler of HCS1.

(11) *********Structures

(12) Number of types of structures

(13) 6

(14) Structure_length (m) Structure iris radius (m) ********COUPLER (PART 1)

(15) 0.0775 0.015

(16) Mode 0 Frequency

(17) 3.00636e+9

(18) For Mode 0, write C if data=R'/Q circuitΩ/m, L if linac, V if loss factor(V/C/m)

(19) V

(20) Corresponding value (set it with – sign for load)

(21) - 9.72e+12

(22) Number of multipoles for 2 π/N fold symmetric structures (0 if symmetric)

(23) 0

(24) Mode 1 Frequency

(25) 4.12e+9

(26) For Mode 1, write C if data=R'/Q circuitΩ/m, L if linac, V if loss factor(V/C)

(27) V

(28) Corresponding value

(29) 15.0e+12

(30) Group_velocity/c Q (attenuation)

(31) 0.001 500.

(32) Number of steps in structure

(33) 8

(34) External source field at beginning of each step + end of last step

(35) 0. –9.25e+6 -18.5e+6 0.0e+6 37.0e+6 74.0e+6 111.0e+6 55.5e+6 0.0e+6

(36) Phase shift bunch 1 (deg)

(37) 60.

(38) d (Phase) per bunch

(39) -0.9574

(40) Structure_length (m) Structure iris radius (m) ********CELL (PART 2)

(41) 0.045704 0.015

(42) Mode 0 Frequency

(43) 3.00636e+9

(44) For Mode 0, write C if data=R'/Q circuitΩ/m, L if linac, V if loss factor(V/C/m)

(45) V

(46) Corresponding value (set it with – sign for load)

(47) -9.72e+12

(48) Number of multipoles for 2 π/N fold symmetric structures (0 if symmetric)

(49) 0

(50) Mode 1 Frequency

(51) 4.12E+9

(52) For Mode 1, write C if data=R'/Q circuitΩ/m, L if linac, V if loss factor(V/C)

(53) V

(54) Corresponding value:

(55) 15+12

(56) Group_velocity/c Q (attenuation)

(57) 0.001 50.

(58) Number of steps in structure

(59) 8

(60) External source field at beginning of each step + end of last step

(61) 0.0e+6.5e+6 37.0e+6 55.5e+6 72.0e+6 55.5e+6 37.0e+6 18.5e+6 0.0e+6

(62) Phase shift bunch 1 (deg)

(63) 60.

(64) d (Phase) per bunch

-0.9574

A.IV. CLIC Decelerator Data (lattice).

The example is given for illustrating the facility of having a loop over a series of elements and for the automatic update of the integrated gradients of the quadrupoles.

The lattice begins at the middle of a quadrupole. Then there are 67 loops over the basic mesh with 2 quadrupoles and 2 structures, then a single mesh. In this single mesh, there are 2 commands for plotting. The loop and the single mesh are repeated 3 other times (not shown). The quadrupoles have a type number indicating if the forces are to be calculated by the automatic procedure, from the first quadrupole of the type, or not.

(1)	50.	0.	0.	1.	
(2)	51.	1.	1.	1.	
(3)	5.0	0.025	-2.64	1.	!half first quadrupole type 1
(4)	3.0	0.1325	0.	0.	
(5)	11.0	0.8	1.	1.	
(6)	3.	0.1325	0.	0.	
(7)	9.0	67.0	0.	0.	!beginning of 67 loops
(8)	5.0	0.05	5.28	2.	!Quad. in the loop, type 2
(9)	50.	0.	0.	1.	
(10)	3.	0.1325	0.	0.	
(11)	11.	0.8	1.	1.	
(12)	3.	0.13250.			0.
(13)	5.	0.05	-5.28	3.	!Quad in the loop, type 3
(14)	50.	0.	0.	1.	
(15)	3.	.1325	0.	0.	
(16)	11.	0.8	1.	1.	
(17)	3.	.1325	0.	0.	
(18)	9.	0.	0.	0.	!end of loops
(19)	5.	0.05	5.28	2.	!Quad type 2
(20)	50.	0.	0.	1.	
(21)	51.	0.	0.	1.	
(22)	3.	.1325	0.	0.	
(23)	11.	0.8	1.	1.	
(24)	3.	0.1325	0.	0.	

(25)	5.	0.05	-5.28	3.	!Quad type 3
(26)	50.	0.	0.	1.	
(27)	51.	0.	0.	1.	
(28)	3.	.1325	0.	0.	
(29)	11.	0.8	1.	1.	
(30)	3.	.1325	0.	0.	